A Journal of the Gesellschaft Deutscher Chemiker

Angewandte International Edition Chemie

GDCh

www.angewandte.org

Accepted Article

Title: Highly ordered self-assembly of native proteins into 1D, 2D and 3D structures modulated by a tether length of inducing ligands

Authors: Guang Yang, Hong-ming Ding, Zdravko Kochovski, Rongting Hu, Yan Lu, Yu-qiang Ma, Guosong Chen, and Ming Jiang

To be cited as: *Angew. Chem. Int. Ed.* 10.1002/anie.201703052
Angew. Chem. 10.1002/ange.201703052

Link to VoR: http://dx.doi.org/10.1002/anie.201703052
http://dx.doi.org/10.1002/ange.201703052

WILEY-VCH

10.1002/anie.201703052

Highly ordered self-assembly of native proteins into 1D, 2D and 3D structures modulated by a tether length of inducing ligands

Guang Yang[a‡], Hong-ming Ding[b‡], Zdravko Kochovski[c‡], Rongting Hu[a], Yan Lu[c,e], Yu-qiang Ma[b,d]*, Guosong Chen[a]*, Ming Jiang[a]

Abstract: Proteins self-assemble into various structures with different dimensions in nature. To construct these nanostructures in laboratories, normally proteins with different symmetries are selected. However, most of these approaches are engineering-intensive and highly dependent on the accuracy of the protein design. In this paper, we report that a simple native protein LecA assembles into one dimensional nanoribbon, nanowire, two dimensional nanosheets as well as three dimensional layered structures controlled mainly by small molecular inducing ligands **RnG** (n=1, 2, 3, 4, 5) with varying number of ethylene oxide repeating units. In order to understand the formation mechanism of the different morphologies controlled by the small molecular structure, molecular simulations were performed from microscopic and mesoscopic view, which presented a clear relationship between the molecular structure of the ligands and the assembled patterns. These results introduce an easy strategy to control assembly structure and dimension, which could shed light on controlled protein assembly in the near future.

Proteins are remarkable building blocks for fabrication of different functional materials due to their enormous structural complexity and intrinsic functions.[1] In nature, proteins self-assemble into different structures in nm or μm scale with highly ordered patterns,[2] e.g. virus capsids, [3] actin filaments, [4] microtubules,[5] bacteria S-layers[6] etc. These attractive structures have stimulated strong motivation for programming proteins into various nano-objects,[7] including oligomers[8[a,b]], zero-dimensional (0D) nanocages,[8b,c] 1D fibers,[9] nanotubes,[10] 2D nanosheets, [11] nanorings[12] and 3D frameworks[13] etc.

However, most natural proteins could be treated as colloidal particles without canonical interacting motifs for precise organization. [2, 14] To achieve regular protein packing structures in laboratory, intensively engineered proteins with well-selected geometry and symmetry are always employed to control protein-protein interactions (PPIs), which highly depended on the accuracy of the protein designs.[15] Unfortunately, in most cases, a single engineered protein building block always leads to only one morphology. In very few elegant designs, metal-ligand interaction has been employed to achieve different assembled structures, [14, 16] but engineered protein building blocks still could not be avoided. Apparently, there is an exceptional challenge to achieve morphologies with different dimensions from one natural protein by slightly tuning the assembly conditions.

Recently, we successfully prepared 3D crystalline frameworks[13b] and 1D helical nanotube[10c] by combining the molecular recognition between lectins and sugars and π–π interactions.. However, in these two reports, concanavalin A (Con A) and soybean agglutinin (SBA) with different shapes were employed to construct the framework and nanotube, separately. In this paper, we demonstrate that by using this strategy, when native protein LecA with cuboid shape[17] is employed as the building block, five kinds of protein assembly structures were obtained by slightly tuning the molecular structure of the inducing ligands and salt concentration. Specifically, only by changing the number of ethylene oxide repeating units from 1 to 5, 1D nanoribbons, nanowires, 2D crystalline nanosheets and 3D layered structures were generated from the same natural protein building block. It is noteworthy that among these structures, the unsupported 2D protein nanosheets with regular spatial arrangements and patterns were the most interesting one,[18] which could not be easily achieved in protein assembly.[19] Moreover, to demonstrate that the significant morphology change of the assemblies was indeed caused by the trivial structure change of the small molecular ligands, all-atom molecular dynamic simulations were employed and the connection between morphology of the assemblies and chemical structure of ligands was revealed.

To achieve a range of morphologies from the same protein, a protein with multiple packing patterns is required. LecA (PA-IL) from *Pseudomonas aeruginosa*, which is a homotetrameric protein with a cuboid-shaped structure (length~7.2 nm, width ~3.5 nm and height ~1.9 nm) is selected as the building block

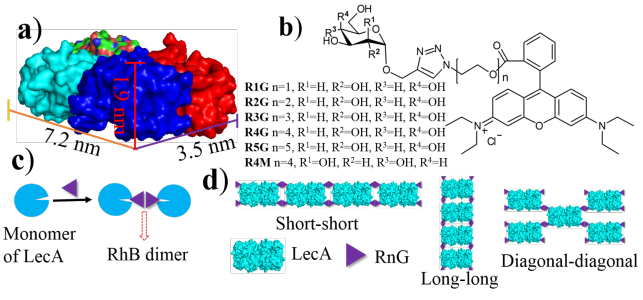

Figure 1. a) Structure of LecA tetramer from Protein Data Bank (PDB code: 4LKD). b) Chemical structures of inducing ligands **RnG** (n = 1 to 5) and **R4M**. c) Driving force of LecA/**RnG** assemblies. d) Three possible packing patterns of LecA/**RnG**.

[a]The State Key Laboratory of Molecular Engineering of Polymers, Department of Macromolecular Science and Collaborative Innovation Center of Genetics and Development, Fudan University, Shanghai 200433, China

[b]Center for Soft Condensed Matter Physics and Interdisciplinary Research, Soochow University, Suzhou 215006, China

[c]Soft Matter and Functional Materials, Helmholtz-Zentrum Berlin für Materialien und Energie, 14109 Berlin, Germany

[d]National Laboratory of Solid State Microstructures and Department of Physics, Collaborative Innovation Center of Advanced Microstructures, Nanjing University, Nanjing 210093, China

[e]Institute of Chemistry, University of Potsdam, 14476 Potsdam, Germany

Corresponding Authors guosong@fudan.edu.cn (G.C.), myqiang@nju.edu.cn (Y. M.)

‡These authors contribute equally to this work.

for assembly fabrication (Figure 1a). LecA is galactose-specific and plays an important role in infection process, especially in biofilm formation.[20] According to our previous reports,[10c, 13b] i.e. proteins are connected via the molecular recognition between lectin and sugar and the π–π stacking of rhodamine B (RhB) between the neighbouring ligands (Figure 1c), five inducing ligands **RnG** (n = 1 to 5) containing Galactopyranoside (Gal) and RhB are prepared with different tether length, i.e. the number of ethylene oxide repeating units varies from 1 to 5 (Figure 1b).. A compound containing RhB but with Mannopyranoside, which does not interact with LecA, replacing Gal was also prepared as a control (**R4M**). Based on the protein packing in crystal structure of LecA-sugar complex,[21] in our design, three kinds of packing patterns formed by LecA with different side length were possible, i.e. short-short, long-long and diagonal-diagonal (Figure 1d).

The condition for LecA/**RnG** assembly was similar ([**RnG**] = 0.1 mM, [LecA] = 0.05 mM (calculated as monomer) in Tris-HCl (25 mM) buffer with [Ca^{2+}] = 0.75 mM, pH 7.5, room temperature).We started with **R1G**, the ligand with the shortest linker. First the self-assembled structure of LecA/**R1G** formed was observed. As shown in Figure 2a, 1D nanoribbon structure was found by transmission electron microscopy (TEM) with negative staining. Under Atomic Force Microscope (AFM), it was quite obvious that the ribbons were formed by a layer of protein protofilaments packing in parallel (Figure 2b). The height of the ribbons was only about 2 nm, which was consistent to the height of a LecA tetramer. The width of each protofilament was just several nanometers, so AFM could not give a precise diameter because of the curvature radius of AFM tip.[22] Then by using negative stained TEM, a single protofilament was clearly observed with a diameter ~3.5 nm, which is closed to the short width of LecA (Figure 2a inset, Figure S1). Meanwhile, the results from cryo-TEM supported the size of protofilaments and their packing into nanoribbon (Figure S2). Combining the above results, the LecA/**R1G** ribbon formation process was proposed in Figure 2c. **R1G** was tethered to the surface of LecA due to the recognition between LecA and Gal, then the RhB moiety on the surface of LecA polymerized resulting the formation of protein protofilament by short-short linkage. The protofilaments further assembled side by side leading to the formation of 1D nanoribbons.

As we mentioned earlier that three different packing styles of LecA/**RnG** are possible. Why did LecA/**R1G** prefer the short-short linkage during the assembly? To answer this question, all-atom molecular dynamics simulation was firstly employed (Figure S3 and the detailed simulation method was in supporting information). To simplify the simulation process, Gal moiety of **R1G** was first placed on the sugar binding sites of LecA and each of the binding sites of one tetramer LecA was made to be occupied. This manipulation was reasonable as in our previous reports, we proved that the binding of sugars to proteins took place before the dimerization of RhB.[13b] Then a couple of LecA/**R1G** complexes (LecA as a tetramer) were initially placed closely, in long-long, diagonal-diagonal and short-short linkages separately (Figure S3b-d). Since the tether length of **R1G** is very short, the π–π stacking between the RhB moieties on neighbouring LecA/**R1G** complexes could be restricted. As a result, long-long linkage would be excluded (Figure 2d), because the neighbouring RhB moieties were far from each other. While for short-short and diagonal-diagonal linkages, π–π stacking between the neighboring RhB was observed (Figure 2e, f). Nevertheless, the diagonal-diagonal linkage was found not stable enough i.e. it may change to different conformations upon time (Figure S4), which made this structure unfavorable for the subsequent packing of proteins. On the contrary, LecA/**R1G** showed easier to pack via the short-short linkage and form the protofilament (Figure 2e). Moreover, the potentials of the mean forces (PMF) for the short-short and diagonal-diagonal packing were calculated. As shown in Figure S5, the energy well in short-short packing was deeper than that of diagonal-diagonal, indicating that this linkage in LecA/**R1G** assembly was energy-favorable. On the basis of above discussion, we summarize that the short-short packing is optimal for LecA/**R1G** assembly. Fortunately, the results from experiment and simulation were consistent to each other, which indicated that the simulation method was reliable to explain the experimental results.

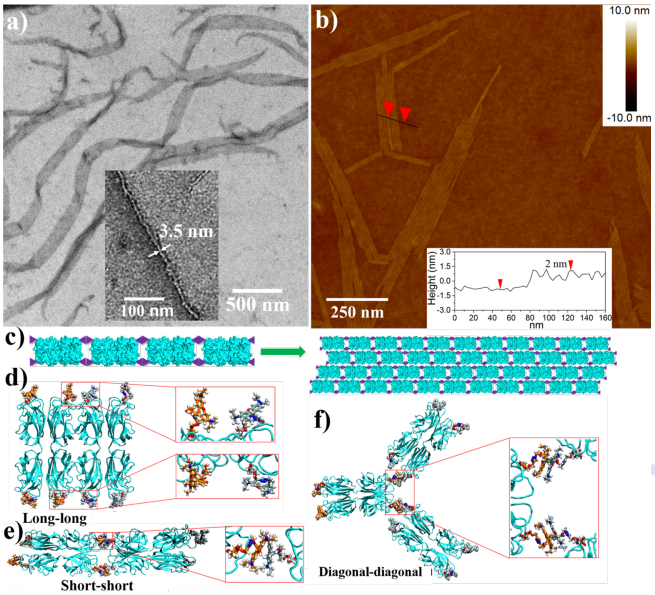

Figure 2. a) TEM micrograph with negative stained LecA/**R1G** assembly (inset: protein protofilament found in some areas). b) AFM micrograph of LecA/**R1G** assembly (inset: height measured along the black line). c) The plausible mechanism of LecA/**R1G** self-assembly. MD simulation result of d) long-long, e) short-short, and f) diagonal-diagonal packing of LecA/**R1G**, in which only the short-short one is possible for large-scale assembly.

Similarly, the self-assembled structure of LecA/**R2G** was observed by cryo-TEM. The results were shown in Figure 3a presenting a clear lattice structure, among which the representative ones marked in the white box were in the size of about 30 nm × 50 nm. In the enlarged photograph (inset image of Figure 3a), the lattice pattern clearly showed that the proteins were connected by the diagonal-diagonal linkage. AFM measurement also revealed that the height of these protein patterns being only about 2 nm (Figure 3b, c), which was consistent to the height of a tetramer LecA, revealing that the nanosheets were made by only one layer of LecA proteins. And for LecA/**R4G** and LecA **R5G**, the same kind of assemblies as LecA/**R2G** was found (Figure 3d-g, Figure S6 and S7). In brief, LecA/**RnG** (n = 2, 4, 5) assembled into 2D nanosheets in a diagonal-diagonal style (Figure 3h). These nanosheets were dispersed in solution unsupported, i.e. free-standing, which was proved by the data from DLS (Figure S8). Synchrotron small-angle X-ray scattering (SAXS) was utilized to further

10.1002/anie.201703052

verify the ordered structure of the 2D LecA/**R4G** assemblies in solution (Figure S9), showing an obvious peak corresponding to the d-space center at about 5 nm, which was consistent to the spacing observed from cryo-TEM (Figure 3e). Furthermore, the π–π stacking between RhB was supported by UV-vis and circular dichroism (CD) spectra (Figure S10a, c, d). DLS and CD (Figure S10b, c) also proved that formation of these 2D lattices was driven by the molecular recognition between LecA/Gal and π–π stacking of RhB. This was proved by the control ligand **R4M** and the dissociation of the assembly after adding the competitive molecules of either free Gal or β-cyclodextrin (β-CD) into the solution. In addition, the isoelectric point (*p*I) of LecA is about 4.9,[20] which indicates that at pH =7.5, LecA exists with negative net charge in aqueous solution. So when the NaCl (from 100 to 400 mM) was added into LecA/**R4G** solution with respect to ion strength, it was found that the 2D nano-sheets stacked into the 3D arrays due to the reduced electrostatic repulsion between different layers (Figure S11 and S12).

To understand why the diagonal-diagonal packing dominates in the cases of LecA/**RnG** (n=2, 4, 5), MD simulation was employed as well. Two LecA/**R2G** complexes were first placed closely via long-long linkages. However, even if they were pushed close, stable structure could not be formed (Figure S13a), since the π–π stacking between the neighboring RhB did not take place, which was very similar to the result of LecA/**R1G**. But when two LecA/**R2G**s were put closely in the short-short and diagonal-diagonal linkages, the π–π stacking between small molecules on different LecA was quickly formed (Figure S13b and Figure 3i). More importantly, here the structure made by diagonal-diagonal linkage changed very little with time (Figure S14), and was more stable compared to that in the case of LecA/**R1G** (Figure S4), which is beneficial for the subsequent packing. Besides, one should notice that although the stable short-short linkage could also occur, our Brownian dynamics (BD) simulations (Figure S15) showed that the structure formed by the short-short linkage was much more flexible than that based on the diagonal-diagonal one (Figure S16). In the research field of supramolecular chemistry, it has been known that relatively rigid linkers do promote the elongation of supramolecular polymers.[23] Considering the possible supramolecular polymeric structure of LecA/**R2G**, it is predictable that the rigid diagonal-diagonal linkage results in larger assemblies. While for **R4G**/**R5G**, in addition to the short-short and diagonal-diagonal linkages, the long-long linkage was also observed (Figure S17 and S18). However, the possible assemblies of LecA/**R4G** or LecA/**R5G** based on the long-long or short-short linkages were soft compared to those formed in the diagonal-diagonal linkages (Figure S16b, c). Similar to the case of **R2G**, the 2D lattice (i.e. diagonal-diagonal linkage) finally won out probably because its high rigidity helped its growth to larger assemblies in the cases of LecA/**R4G** and LecA/**R5G**.

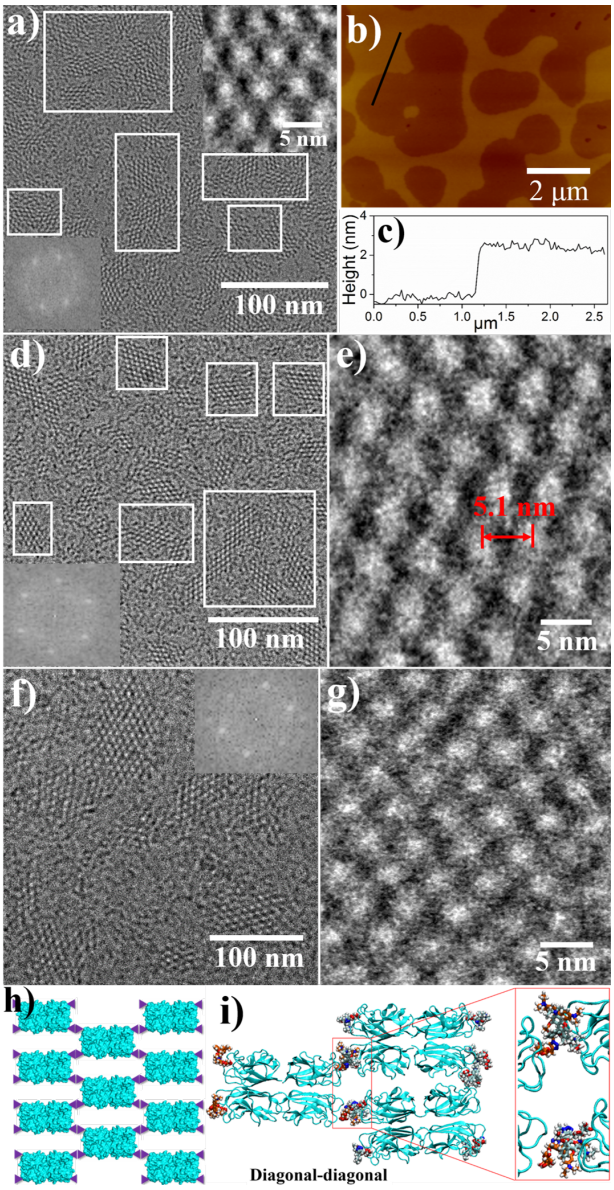

Figure 3. a) Cryo-TEM micrograph (inset: enlarged cryo-TEM micrograph of the nanosheet and Fourier-transform image) and b) AFM image of 2D LecA/**R2G** lattice. c) The height of LecA/**R2G** nanosheet along the black line in b). d) Cryo-TEM (inset: Fourier-transform image) and e) enlarged cryo-TEM micrographs of 2D LecA/**R4G** nanosheet. f) Cryo-TEM (inset: Fourier-transform image) and g) enlarged cryo-TEM micrographs of 2D LecA/**R5G** nanosheet. h) The plausible assemblied mechanism of LecA/**RnG** (n= 2, 4, or 5) 2D nanosheet. i) MD simulation result of diagonal-diagonal packing of LecA/**R2G**.

Very interestingly, the assembly of LecA/**R3G** presented a unique morphology differing from the 1D nanoribbons and 2D nanosheets mentioned above. First of all, DLS revealed that self-assembly of LecA and **R3G** took place (Figure S19). TEM with negative staining revealed that the morphology of LecA/**R3G** assembly was 1D nanowire with a width about 21 nm (Figure 4a), which of course was far from a single protein protofilament. In fact, at the end of the nanowire, several slim protofilaments were observed (Figure 4b) with width about 9 nm, which was close to the long side width of LecA tetramer. This observation indicated that the nanowires were made by slim protofilaments (formed via length-length linkage) twisting together. Cryo-TEM also supported the morphology of

nanowire (Figure 4c, S20). Fortunately, in some areas, the single protofilament can be observed clearly. Under cryo-TEM, the width of the nanowire was about 19 nm while the width of the protofilament was about 7.4 nm (Figure 4d), which is consistent with the long size width of LecA. The diameters of the nanowires and the protofilaments measured by cryo-TEM were slightly smaller than those measured under negative staining, which was reasonable due to the collapsed state of materials under high vacuum. Based on these data, we proposed that the nanowires were formed by several protein protofilaments, while every protofilament was formed by LecA in a long-long linkage (Figure 4e). In this case, MD simulations were also used to reveal the possibility of three packing styles. Different from the case of LecA/**R1G** and LecA/**R2G** due to the long length of **R3G**, in addition to the short-short and diagonal-diagonal linkage (Figure S21a and b), here the long-long linkage can also occur (Figure S21c). In this sense, the packing styles here are similar to the case of LecA/**R4G** and LecA/**R5G**. However, since the tether length of **R3G** is shorter compared to those of **R4G** and **R5G**, the rigidity of the assembly of LecA/**R3G** with long-long linkage is close to that of the corresponding assemblies of **R4G** and **R5G** (Figure S16), which might be the reason for the nanowire in a long-long linkage. However, when the concentration of NaCl was increased to more than 100 mM, the packing style of LecA/**R3G** became diagonal-diagonal and also formed **3D** layerd structures (Figure S22, S23).

In summary, we demonstrated that different morphologies from 1D nanoribbon, nanowire, to 2D nanosheet and 3D layered structure were easily achieved by LecA/**RnG** when the linker length of the inducing ligand **RnG** was slightly changed. In this cases, native protein LecA was used, no molecular engineering on the protein was required. The success of this assembly not only demonstrated the beauty of the dual non-covalent interactions, i.e. lectin-sugar interaction and π–π stacking in the field of protein self-assembly, but also showed that accurate structural control of the inducing ligand did play crucial roles in the assembly process. By controlling the salt concentration, the electrostatic interaction between the negatively charged proteins and the RhB groups with positive charge might also contribute to the assembly process, which deserves deep discussion in our future research. This simple approach of building protein assemblies with different dimensions will be useful to prepare various functional materials with precise structure and well-controlled morphology.

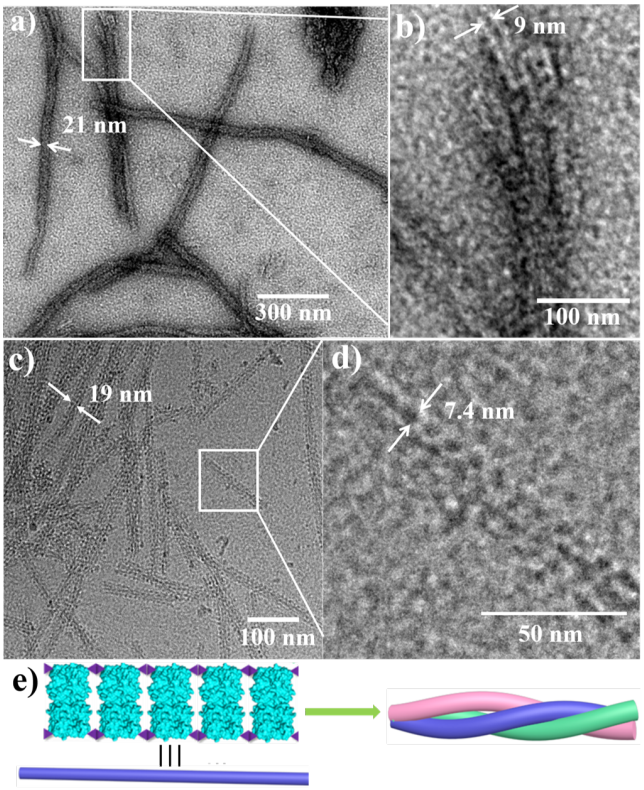

Figure 4. a-b) Negative stained TEM and c-d) cryo-TEM micrographs of LecA/**R3G** assembly. e) Possible mechanism of LecA/**R3G** assembly.

Acknowledgements

We thank National Natural Science Foundation of China (No. 21504016, 91527305 and GZ962), National Center for Protein Science Shanghai (Cryo-TEM) and Shanghai Synchrotron Radiation Facility (synchrotron SAXS, and Joint Lab for Structural Research at the Integrative Research Institute for the Sciences),

Keywords: Protein self-assembly •carbohydrate-protein interaction • dual non-covalent interaction • molecular simulation

References:

[1] a) T. Ueno, *Chem.–Eur. J.* **2013**, *19*, 9096-9102; b) G. Yang, L. Wu, G. Chen, M. Jiang, *Chem. Commun.* **2016**, *52*, 10595-10605.
[2] B. J. G. E. Pieters, M. B. Van Eldijk, R. J. M. Nolte, J. Mecinovic, *Chem. Soc. Rev.* **2016**, *45*, 24-39.
[3] J. M. Alonso, M. Ł. Górzny, A. M. Bittner, *Trends Biotechnol.* **2013**, *31*, 530-538.
[4] A. Mogilner, G. Oster, *Biophys. J.* **1996**, *71*, 3030-3045.
[5] M. A. Jordan, L. Wilson, *Nat. Rev. Cancer* **2004**, *4*, 253-265.
[6] S. Scheuring, H. Stahlberg, M. Chami, C. Houssin, J. L. Rigaud, A. Engel, *Mol. Microbiol.* **2002**, *44*, 675-684.
[7] a) E. N. Salgado, R. J. Radford, F. A. Tezcan, *Acc. Chem. Res.* **2010**, *43*, 661-672; b) Y. Bai, Q. Luo, J. Liu, *Chem. Soc. Rev.* **2016**, *45*, 2756-2767; c) O. Koji, O. Akira, H. Takashi, *Chem. Commun.* **2012**, *48*,11714-11726; d) T. O. Yeates, Y. Liu, J. Laniado, *Curr. Opin. Struct. Biol.* **2016**, *39*, 134-143.
[8] a) R. E. Mcgovern, A. A. Mccarthy, P. B. Crowley, *Chem. Commun.* **2014**, *50*, 10412-10415; b) M. L. Rennie, A. M. Doolan, C. L. Raston, P. B. Crowley, *Angew. Chem., Int. Ed.* **2017**, *56*, 5517-5521; c) J. E. Padilla, C. Colovos, T. O. Yeates, *Proc. Natl. Acad. Sci. U. S. A* .**2001**, *98*, 2217-2221; d) N. P. King, J. B. Bale, W. Sheffler, M. N. Dan, S. Gonen, T. Gonen, T. O. Yeates, D. Baker, *Nature* **2014**, *510*, 103-108.
[9] a) C. Hou, J. Li, L. Zhao, W. Zhang, Q. Luo, Z. Dong, J. Xu, J. Liu, *Angew. Chem., Int. Ed.* **2013**, *52*, 5590-5593; b) W. Zhang, Q. Luo, L. Miao, C. Hou, Y. Bai, Z. Dong, J. Xu, J. Liu, *Nanoscale* **2012**, *4*, 5847-5851; c) H. Kitagishi, K. Oohora, H. Yamaguchi, H. Sato, T. Matsuo, A. Harada, T. Hayashi, *J. Am. Chem. Soc.* **2007**, *129*, 10326-10327.

10.1002/anie.201703052

[10] a) J. D. Brodin, S. J. Smith, J. R. Carr, F. A. Tezcan, *J. Am. Chem. Soc.* **2015**, *137*, 10468-10471; b) S. Biswas, K. Kinbara, N. Oya, N. Ishii, H. Taguchi, T. Aida, *J. Am. Chem. Soc.* **2009**, *131*, 7556-7557; c) G. Yang, Z. Xiang, Z. Kochovski, Y. Zhang, B. Dai, F. Sakai, J. Lin, L. Yan, M. Ballauff, X. Li, C. Liu, G. Chen, M. Jiang, *J. Am. Chem. Soc.* **2016**, *138*, 1932-1937.
[11] a) Y. Suzuki, G. Cardone, D. Restrepo, P. D. Zavattieri, T. S. Baker, F. A. Tezcan, *Nature* **2016**, *533*, 369-373; b) S. Gonen, F. Dimaio, T. Gonen, D. Baker, *Science* **2015**, *348*, 1365-1368; c) Y. N. Kim, Y. Jung, *Org. Biomol. Chem.* **2016**, *14*, 5352-5356; c) Sarah M. Dimick, Steven C. Powell, Stephen A. McMahon, Davina N. Moothoo, James H. Naismith, Eric J. Toone, *J. Am. Chem. Soc.* **2000**, *121*,10286-10296.
[12] a) T. F. Chou, C. So, B. R. White, J. C. Carlson, M. Sarikaya, C. R. Wagner, *ACS Nano* **2008**, *2*, 2519-2525; b) Y. Bai, Q. Luo, W. Zhang, L. Miao, J. Xu, H. Li, J. Liu, *J. Am. Chem. Soc.* **2013**, *135*, 10966-10969.
[13] a) P. A. Sontz, J. B. Bailey, S. Ahn, F. A. Tezcan, *J. Am. Chem. Soc.* **2015**, *137*, 11598-11601; b) F. Sakai, G. Yang, M. S. Weiss, Y. Liu, G. Chen, M. Jiang, *Nat. Commun.* **2014**, *5*, 4634; c) Y. T. Lai, E. Reading, G. L. Hura, K. L. Tsai, A. Laganowsky, F. J. Asturias, J. A. Tainer, C. V. Robinson, T. O. Yeates, *Nat. Chem.* **2014**, *6*, 1065-1171; d) V. Liljeström, J. Mikkilä, M. A. Kostiainen, *Nat. Commun* **2014**, *5*, 5445; e) M. Künzle, T. Eckert, T. Beck, *J. Am. Chem. Soc.* **2016**, *138*, 12731-12734.
[14] J. D. Brodin, J. R. Carr, P. A. Sontz, F. A. Tezcan, *Proc. Natl. Acad. Sci. U. S. A.* **2014**, *111*, 2897-2902.
[15] a) C. S. Zhang, L. H. Lai, *Acta Phys.-Chim. Sin.* **2012**, *28*, 2363-2380; b) J. C. Sinclair, K. M. Davies, C. Vénienbryan, M. E. M. Noble, *Nat. nanotechnol.* **2011**, *6*, 558-562.
[16] a) J. D. Brodin, X. I. Ambroggio, C. Tang, K. N. Parent, T. S. Baker, F. A. Tezcan, *Nat. Chem.* **2012**, *4*, 375-382; b) S. P. Qiao, C. Lang, R. D. Wang, X. M. Li, T. F. Yan, T. Z. Pan, L. L. Zhao, X. T. Fan, X. Zhang, C. X. Hou, *Nanoscale* **2016**, *8*, 333-341.
[17] V. Wittmann, R. J. Pieters, *Chem. Soc. Rev.* **2013**, *42*, 4492-4503.
[18] S. Z. Butler, S. M. Hollen, L. Cao, Y. Cui, J. A. Gupta, H. R. Gutiérrez, T. F. Heinz, S. S. Hong, J. Huang, A. F. Ismach, *ACS Nano* **2013**, *7*, 2898-2926.
[19] Q. Luo, C. Hou, Y. Bai, R. Wang, J. Liu, *Chem. Rev.* **2016**, *116*, 13571-13632.
[20] A. Imberty, M. Wimmerová, E. P. Mitchell, N. Gilboagarber, *Microbes and Infect.* **2004**, *6*, 221-228.
[21] a) R. U. Kadam, M. Bergmann, D. Garg, G. Gabrieli, A. Stocker, T. Darbre, J. L. Reymond,*Chem.– Eur. J.* **2013**, *19*, 17054-17063; b) A. Novoa, T. Eierhoff, J. Topin, A. Varrot, S. Barluenga, A. Imberty, W. Römer, N. Winssinger, *Angew. Chem., Int. Ed.* **2014**, *53*, 8885-8889.
[22] D. Sicard, S. Cecioni, M. Iazykov, Y. Chevolot, S. E. Matthews, J. P. Praly, E. Souteyrand, A. Imberty, S. Vidal, M. Phanergoutorbe, *Chem. Commun.* **2011**, *47*, 9483-9485.
[23] J. F. Xu, L. Chen, X. Zhang, *Chem.–Eur. J.* **2015**, *21*, 11938-11946.

10.1002/anie.201703052

COMMUNICATION

Guang Yang[a‡], Hong-ming Ding[b‡], Zdravko Kochovski[c‡], Rongting Hu[a], Yan Lu[c,e], Yu-qiang Ma[b,d]*, Guosong Chen[a]*, Ming Jiang[a]

Highly ordered self-assembly of native proteins into 1D, 2D and 3D structures modulated by a tether length of inducing ligands